FINAL REPORT

Magnetically Activated Self-Cleaning Membranes

SERDP Project WP-1670

JUNE 2010

S. Ranil Wickramasinghe
Dr. Xianghong Qian
Colorado State University

SERDP
DOD ▪ EPA ▪ DOE

Report Documentation Page

Form Approved
OMB No. 0704-0188

1. REPORT DATE	2. REPORT TYPE	3. DATES COVERED
JUN 2010		**00-00-2010 to 00-00-2010**

4. TITLE AND SUBTITLE	5a. CONTRACT NUMBER
Magnetically Activated Self-Cleaning Membranes	5b. GRANT NUMBER
	5c. PROGRAM ELEMENT NUMBER
6. AUTHOR(S)	5d. PROJECT NUMBER
	5e. TASK NUMBER
	5f. WORK UNIT NUMBER
7. PERFORMING ORGANIZATION NAME(S) AND ADDRESS(ES) **Colorado State University,Fort Collins,CO,80523**	8. PERFORMING ORGANIZATION REPORT NUMBER
9. SPONSORING/MONITORING AGENCY NAME(S) AND ADDRESS(ES)	10. SPONSOR/MONITOR'S ACRONYM(S)
	11. SPONSOR/MONITOR'S REPORT NUMBER(S)

12. DISTRIBUTION/AVAILABILITY STATEMENT
Approved for public release; distribution unlimited

13. SUPPLEMENTARY NOTES

14. ABSTRACT

Membrane fouling, due to deposition of particulate matter on the surface of the membrane and concentration polarization, limits the use of membranes for water treatment. Mixing at the membrane interface can suppress deposition of particulate matter and break up the concentration boundary layer. We hypothesize that movement of magnetically activated polymer brushes on the membrane surface will create mixing at the membrane interface that suppresses fouling. Commercially available nanofiltration membranes were modified by growing polymer brushes from the surface of the membrane. Two different polymerization methods have been developed: UV initiated free radical polymerization and atom transfer radical polymerization. Superparamagnetic nanoparticles were attached to the polymer brushes. In an oscillating magnetic field the brushes oscillate leading to mixing at the membrane surface. Particle image velocimetry has been used to visualize this mixing by comparing the velocity field in the presence and absence of an oscillating magnetic field for nonmodified and modified membranes. Magnetically activated nanobrushes induce mixing at the membrane surface. Moreover, the degree of mixing depends critically on the external field frequency. Filtration experiments were conducted using feed streams of DI water containing polyamide particles and hand soap. Permeate flux and rejection of the hand soap were significantly improved in the presence of an oscillating magnetic field for modified membranes. These results indicate that magnetically responsive brushes may be grafted to the surface of membranes. In an oscillating magnetic field movement of the brushes suppresses fouling and concentration polarization leading to enhanced performance and increased lifetime of membranes.

15. SUBJECT TERMS

16. SECURITY CLASSIFICATION OF:			17. LIMITATION OF ABSTRACT	18. NUMBER OF PAGES	19a. NAME OF RESPONSIBLE PERSON
a. REPORT **unclassified**	b. ABSTRACT **unclassified**	c. THIS PAGE **unclassified**	**Same as Report (SAR)**	**34**	

Table of Contents

List of Tables

List of Figures

List of Acronyms & Terminology

1:15 : Membrane modified using 1% acrylic acid solution for 15 minutes
2:10 : Membrane modified using 2% acrylic acid solution for 10 minutes
2:15 : Membrane modified using 2% acrylic acid solution for 15 minutes
ATR-FTIR: Attenuated total reflectance - Fourier transform infrared
ATRP: Atom transfer radical polymerization
BPY: Bipyridine
DI Water: Deionized water
DMAP: 4-n'n'-dimethylaminopyridine
DMF: n,n-dimethylformamide
EDC: 1-ethyl-3-(3-dimethylaminopropyl) carbodiimide
HEMA: 2-hydroxyethylmethacrylate
NF: Nanofiltration
NHS: n-hydroxysuccinimide
pAA: Poly acrylic acid
pHEMA: Poly HEMA
PIV: Particle imaging velocimetry
PLC: Programmable logic controller
PMDETA: N-N-N-N-N-Pentamethyldiethylenetriamine
SEED: SERDP Exploratory Development
SERDP: Strategic Environmental Research and Development Program
TEA: Triethylamine
UV: Ultraviolet
XPS: X-ray photoelectron spectroscopy

Keywords

Bilge water, flux, fouling, membrane modification, mixing, nanofiltration, oily wastewaters, rejection, superparamagnetic nanoparticles

Acknowledgements

The financial support of the Strategic Environmental Research and Development Program is acknowledged. In addition, the authors would like to thank Mr. Heath H. Himstedt, Prof. Prasad Dasi, Prof. Michael Semmens, Prof. Mathias Ulbricht, and Dr. Qian Yang.

Abstract

Membrane fouling, due to deposition of particulate matter on the surface of the membrane and concentration polarization, limits the use of membranes for water treatment. Mixing at the membrane interface can suppress deposition of particulate matter and break up the concentration boundary layer. We hypothesize that movement of magnetically activated polymer brushes on the membrane surface will create mixing at the membrane interface that suppresses fouling. Commercially available nanofiltration membranes were modified by growing polymer brushes from the surface of the membrane. Two different polymerization methods have been developed: UV initiated free radical polymerization and atom transfer radical polymerization. Superparamagnetic nanoparticles were attached to the polymer brushes.

In an oscillating magnetic field the brushes oscillate leading to mixing at the membrane surface. Particle image velocimetry has been used to visualize this mixing by comparing the velocity field in the presence and absence of an oscillating magnetic field for non-modified and modified membranes. Magnetically activated nanobrushes induce mixing at the membrane surface. Moreover, the degree of mixing depends critically on the external field frequency. Filtration experiments were conducted using feed streams of DI water containing polyamide particles and hand soap. Permeate flux and rejection of the hand soap were significantly improved in the presence of an oscillating magnetic field for modified membranes.

These results indicate that magnetically responsive brushes may be grafted to the surface of membranes. In an oscillating magnetic field movement of the brushes suppresses fouling and concentration polarization leading to enhanced performance and increased lifetime of membranes.

Objective

The proof of concept work conducted here directly addresses the Navy's need to treat shipboard wastewaters. The proposed work represents a highly innovative approach to address membrane fouling by suspended solids and oils. Previous studies have shown that base nanofiltration (NF) membranes may be grafted with nanobrushes forming a polymer nanolayer that responds to an external stimulus such as temperature, pH or ionic strength [1, 2]. Here magnetically responsive nanobrushes are attached to base NF membranes. In an oscillating magnetic field, movement of the brushes suppresses membrane fouling and concentration polarization. This, in turn, will lead to improved membrane performance, higher membrane capacity, and less frequent cleaning. In addition, our solution to membrane fouling has a similar foot print to current equipment, is light weight, can be automatically cleaned in place, and represents a non mechanical solution. This proof of concept research can be broken down into 4 specific objectives:

1) Can magnetic nanoparticles be attached to the surface of membranes via polymeric nanobrushes?
2) Can these magnetic nanobrushes induce local mixing at the surface of attachment?
3) How is the induced mixing impacted by the design of the magnetic nanobrushes and the applied magnetic field? How do coatings used to protect the nanoparticles, and strength and oscillation frequency of the external field impact performance?
4) How does induced mixing impact performance of the nanofiltration membrane?

The results of this SEED project successfully answer the questions posed by these four objectives. Superparamagnetic nanoparticles may be attached to commercially available nanofiltration membranes. In an oscillating magnetic field, we show that the magnetically active polymer brushes induce movement of water at the membrane surface. Thus, the attachment protocols we have developed for growing polymer brushes from the membrane surface and attaching the nanoparticles to the polymer brushes results in brushes that are able to move in an oscillating magnetic field. Theoretical calculations support these experimental findings.

Dead end filtration experiments indicate that movement of the magnetically responsive nanobrushes leads to enhanced permeate fluxes and improved rejection by the membrane due to reduced deposition of insoluble particulate matter and suppression of concentration polarization. The results of this project are significant for a number of reasons and provide a strong foundation for further investigation. The initial hypothesis, that magnetically responsive membranes are fouling resistant, is validated.

Background

Treatment technologies for wastewaters often fail due to the presence of emulsified oils and suspended solids[3]. Wastewaters of interest to the Navy include graywater and bilge water. Bilge water often consists of an oil-water emulsion which may contain a number of suspended solids and chemicals, such as detergents[4]. Several investigators have

considered the use of membranes for treatment of oily waters[4,5,6,7,8]. The Navy currently uses membrane filtration as part of its water treatment operations to ensure water discharged from ships meets effluent discharge requirements; however, the Navy is seeking more robust alternative technologies, which could better handle wastewaters.

Membrane fouling limits membrane selectivity, capacity and throughput[9]. Reducing membrane fouling would greatly improve membrane performance and allow for extended use before cleaning and/or replacement. This is especially true for highly-fouling streams such as bilge and graywaters, which can quickly and irreversibly foul membranes. Presented here is a truly novel approach to reducing fouling due to colloids and oils present in aqueous feeds: magnetically-responsive membranes. Polymer chains have been grafted onto the surface of nanofiltration (NF) membranes using either UV-initiated free radical polymerization or atom transfer radical polymerization (ATRP). The polymer brushes were then capped with superparamagnetic nanoparticles. We have shown that these nanoparticles align and move in response to an alternating external magnetic field as schematically seen from Figure 1. The resulting movement of the polymer brushes induces mixing at the membrane surface. This reduces membrane fouling, thereby increasing membrane lifetime. Nanofiltration membranes were chosen because they are widely used in water filtration applications; however, our membranes are truly unique in that no published studies have investigated using magnetically-responsive membranes to generate mixing and hence suppress fouling [10,11,12]. Our proposed technology has demonstrated tremendous potential and validated this proof-of-concept study. Improved membrane performance was verified using model systems. The next stage of this research would be the construction and testing of a system that accurately represents filtration systems used by the Navy. Such a system would be tested with real bilge waters.

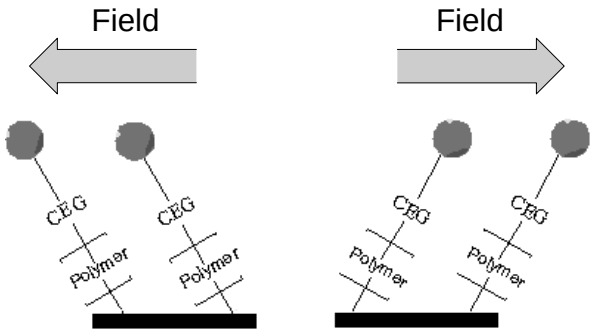

Figure 1. The nanoparticle-capped polymer brushes align with an external magnetic field. By applying an alternating field, these brushes will move and induce mixing at the membrane surface.

A breakdown of the tasks and completion dates of each task is given in Table 1 below.

Table 1. Description of project tasks and completion dates

Task #	Task Name	Subtask (milestone)	Completion
1	Selection of magnetic nanoparticles		Sep-09
1.1		Establish system to generate oscillating magnetic field	May-09
2	Modification of commercial nanofiltration membranes		Mar-10
3	Characterization and visualization of modified membranes		Mar-10
3.1		Determine permeate flux for modified membranes	Mar-10
3.2		Visualize nanobrush movement	Mar-10
4	Compare modified and unmodified membranes	Data indicating superior performance of modified membranes	Apr-10
5	Submit technical reports		May-10
5.1		Submit draft final technical report	Jun-10
5.2		Submit final technical report	Jun-10

The major challenges that represented the greatest risk were:

(i) Demonstration of our ability to attach superparamagnetic particles to polymer brushes grown from the membrane surface
(ii) Demonstration that these magnetically responsive brushes are able to move in an oscillating magnetic field
(iii) Demonstration that this movement will induce mixing at the member interface and hence improve membrane performance (flux and rejection).

Our preliminary results demonstrate all of the above, provide all the required preliminary proof of concept data, and significantly reduce any initial risk associated with this new technology.

Materials and Methods

Chemicals

NF 270 membranes (Dow, Midland, MI) were supplied by the manufacturer. This is a semi-aromatic poly(piperazinamide) membrane formed by piperazine and trimesoyl chloride[13]. The thin piperazine-based semi-aromatic polyamide barrier layer is cast on top of polysulphone and polyester support layers which provide mechanical support for the membrane. All purified water (DI water) was obtained from a Siemens/ELGA Purelab Ultra deionizer and filter (SCMK2) from Siemens Water Technologies (Warrendale, PA). Unless otherwise noted, all chemicals were reagent grade. Acetonitrile, benzophenone, calcium chloride, magnesium sulfate, sodium hydroxide, and sulfuric acid were purchased from ThermoFischer Scientific (Waltham, MA); n,n-dimethylformamide (DMF) was from Acros Organics (Morris Plains, NJ); potassium permanganate, diisopropylcarbodiimide, n-hydroxybenzotriazole, ethanolamine, triethylamine (TEA), N-N-N-N-N-Pentamethyldiethylenetriamine (PMDETA), and 4-n'n'-dimethylaminopyridine (DMAP) were from Fluka (St. Louis, MO); methanol (85%) from Mallinckrodt Chemicals (Phillipsburg, NJ); α-bromoisobutyrlbromide, 2-hydroxyethylmethacrylate (HEMA), 1-ethyl-3-(3-dimethylaminopropyl)carbodiimide (EDC), n-hydroxysuccinimide (NHS), acrylic acid, sodium azide, bipyridine (BPY Reagent Plus) and hydrochloric acid (37%) from Sigma-Aldrich Corp. (St. Louis, MO); ethanol from Pharmco-Aaper (Brookfield, CT); and polyamide 20 μm neutrally buoyant seeding particles were from Dantech Dynamics (Skovlunde, Denmark). Magnetite Fe_3O_4 superparamagnetic nanoparticles (15 nm diameter core size, 5 nm coating layer functionalized with carboxylic acid or amine) were purchased from Ocean Nanotech (Fayetteville, AR, USA).

Surface Modification via UV-initiated polymerization

Benzophenone, a type II photoinitiator, was dissolved to saturation in DI water at room temperature. Acrylic acid monomer was then added resulting in solutions that were 1 or 2%, by weight, acrylic acid. The acrylic acid solution was then purged with nitrogen gas for 15 minutes. Membrane discs (25 mm diameter), cut from a larger membrane sheet, were placed in a 15 mL Petri dish and the purged benzophenone-saturated monomer solution (5 mL) was added. A piece of filter paper was placed on top of the membrane, and the cover of the Petri dish was inverted and placed on top of the filter paper to force out any air bubbles in the reaction solution. The Petri dish "sandwich" was then placed in the UV reactor. The membranes were incubated in the monomer solution for 15 minutes before the UV source, a Hoenle UV irradiation system (Gräfelfing, Germany), was turned on. The average intensity falling on the membrane (covered with filter paper) was ~13 mW/cm^2. Membranes in 1% acrylic acid solution were irradiated for 15 minutes, while membranes in 2% acrylic acid solution were irradiated for either 10 or 15 minutes. Multiple membrane samples were modified at each condition.

Following irradiation, the membranes were rinsed twice with 10 mL DI water. They were then placed in a 100 mL beaker containing 50 mL DI water at room temperature for 30 minutes with slow stirring. Next, the membranes were washed for 60 minutes with 50 mL DI water of 45°C and 50 mL of room temperature DI water, both in 100 ml beakers with

slow stirring. The membranes were again rinsed twice with 10 mL DI water and air dried for 15 minutes. They were then placed in an oven at 40°C for 6 hours. Membranes were stored in a refrigerator in zip top bags containing 0.01 wt% sodium azide solution to prevent bacterial growth during storage.

Surface Modification via ATRP

Initiator Immobilization

A solution containing the ATRP initiator was prepared by adding 1.515 g TEA, 91.5 mg DMAP, and 2.76 g α-bromoisobutyrylbromide to 150mL of dried acetonitrile. The membrane disks were placed in small glass vials to which 5 mL of this reaction solution was added. The membranes were allowed to react for 2 hours at room temperature on a shaker table. The membrane was then washed with acetonitrile (once) methanol (twice), and deionized water (twice). In each case 5 mL of the liquid used to wash the membrane was placed in the glass vial and the membrane was incubated in the liquid for 1 minute. The membranes were then dried overnight at 40°C. The membranes were then weighed.

Surface initiated ATRP of HEMA

The reaction solution for ATRP grafting consisted of purified, distilled HEMA monomer (2M), CuCl, $CuCl_2$, and BPY Reagent Plus dissolved in equal parts water and methanol. The ratios used were 100 : 0.5 : 0.1 : 1.5 corresponding to monomer : CuCl : $CuCl_2$: BPY Reagent Plus. First, a 100 mL mixture of 50% (v/v) methanol in water was prepared. A total of 24.257 mL purified HEMA monomer was added and the solution was degassed while stirring for 5 minutes with nitrogen. Then 468 mg of BPY Reagent Plus was added, and degassing continued for 15 minutes. The vials containing the membrane disks were then evacuated under vacuum and then filled with nitrogen. The process was repeated two more times to ensure an oxygen free environment. Then 98.99 mg of CuCl was added to the reaction solution. The solution was degassed for 10 minutes before the addition of 26.89 mg of $CuCl_2$. The solution was degassed for another 10 minutes. Immediately after this, 6 mL of reaction solution was injected into each of the sealed vials containing the membrane disks. The membranes were allowed to react for various times at room temperature.

After reaction, the membranes were placed in a quenching solution to halt polymerization and cap the end of each polymer chain with a bromine group. To prepare the quenching solution, 500 mg of $CuBr_2$ and 1250 μL of PMDETA were dissolved in 100mL of 50% (v/v) methanol and water. After shaking for 10 minutes in the quenching solution the membranes were washed with DI water for 2 minutes, methanol for 1 minute, and finally soaked in DI water for 2 hours. The membranes were then dried in a 40°C oven overnight and then massed.

Gabriel Synthesis Procedure

After soaked in the quenching solution, the polymer brushes were capped with bromine and need to be functionalized in order to react with the carboxylic acid coated nanoparticles. In order to create a covalent amide linkage between the end of the polymer nanobrush and the nanoparticle, it is necessary to convert the alkyl halide polymer brush

ends to a primary amine through the Gabriel Synthesis[14]. Briefly, potassium phthalimide was reacted with the brushes to attach the phthalimide group to the end of the brushes. Hydralization then yields a primary amine. The phthalimide by-product is precipitated and washed away. The reaction is shown schematically in Figure 2.

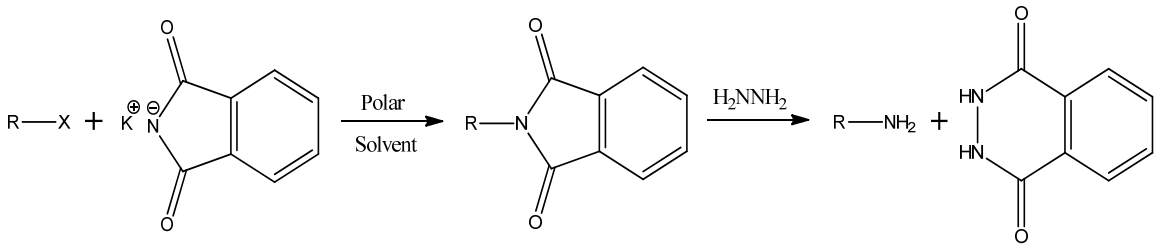

Figure 2. Overview of Gabriel Synthesis reaction

For the first step of the Gabriel Synthesis, 1 g potassium phthalimide was dissolved into 20 mL of ethanol. This solution (4.5 mL) was placed into a small glass vial containing one membrane disk. The vials were sealed and placed in a 40^{o}C oil bath for 6 hours. After reaction, the membrane was rinsed with DMF followed by DI water twice for two minutes, and finally ethanol before being dried and weighed.

The second step of the Gabriel Synthesis consisted of dissolving 7 mL of hydrazine hydrate into 25 mL of 6M HCl. This solution (4 mL) was placed in a small glass vial containing a membrane disk. The vials were placed in a 40^{o}C oil bath for 6 hours. Upon completion of the reaction, the third step (washing) was performed. The membrane was washed twice with DI water, once with methanol, again with DI water, once with ethanol, and finally with DI water to ensure that no phthalimide precipitate remained. The membranes were then dried and weighed.

Nanoparticle Attachment

Superparamagnetic magnetite (Fe_3O_4) nanoparticles were purchased from the Ocean Nanotech, LLC. The diameter of the particles is 25 nm which includes a 15 nm magnetic core and 5 nm thick coating layer. The surfaces of the nanoparticles are amine or carboxylic acid functionalized. The nanoparticle attachment method was the same for polymer brushes grown using UV initiated polymerization or ATRP; the only difference being the functional groups on the nanoparticle. EDC (31.2 mg) and NHS (38.7 mg) were added to 10 mL DI water and shaken vigorously using a vortex mixer. Then 0.3 mL superparamagnetic nanoparticles in buffer solution (5g/L) were added, but not agitated. 1.5 mL of this solution was then added to a plastic jar containing a membrane. This was sealed and incubated in the dark for 4 hours. After incubation, the membrane was removed, washed twice in DI water for 5 minutes, then with ethanol, and finally in DI water for 10 minutes. The membrane was then dried overnight at 40^{o}C. The magnetic nanoparticles were attached to the polymer brushes through the creation of an amide linkage. For UV-initiated grafting, the carboxylic acid at the end of the pAA brushes bound with the amine coating of the particles, and carboxylic acid coated particles bound to the amine end functionality of the HEMA brushes grafted using ATRP. A visual representation of the modification scheme is shown in Figure 3.

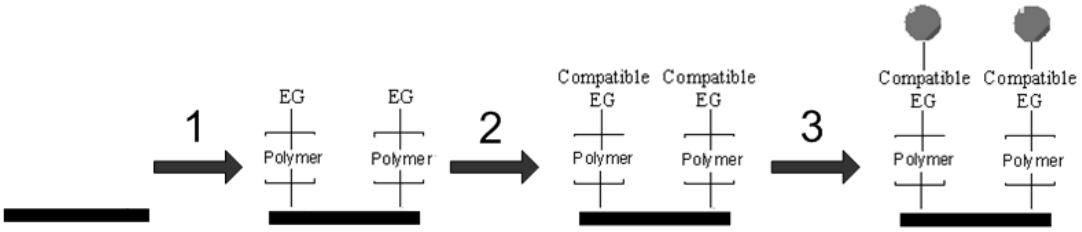

Figure 3. Schematic of modification scheme. Polymer brushes are grown from the membrane surface using either UV polymerization or ATRP. In the case of ATRP, the end group (EG) of the polymer must be converted to a compatible end group (amine) before attachment of the nanoparticles. This end group conversion is not required for UV polymerization.

Membrane Characterization

X-ray Photoelectron Spectroscopy (XPS)

XPS provides chemical binding information for the top 1-10 nm of the sample[15]. Membranes were washed twice with DI water and dried before analysis. For each sample, 10 survey scans at a 45° take-off angle over the range 0-1100 eV with a resolution of 1 eV were averaged using a Physical Electron 5800 ultra-high vacuum XPS-Auger spectrometer (Chanhassen, MN). Additionally, 20 scans focusing on the carbon (282-292 eV), nitrogen (394-406 eV), sulfur (164-174), and iron (705-730) regions were averaged to observe changes during sequential modification steps.

Attenuated Total Reflectance Fourier Transform Infrared (ATR-FTIR) Spectroscopy

ATR-FTIR spectroscopy provides qualitative information on the types of functional groups present at depths between 100 and 1000 nm[19]. Membranes were washed twice with DI water and dried before analysis. A Nicolet Magna 760 FTIR spectrometer, Thermo Electron Corporation (Madison, WI) equipped with a mercury-cadmium-tellurium (MCT) detector with a resolution of 4 cm^{-1} and zinc selenide (ZnSe) crystal plate with an incidence angle of 45° was used. Spectra were averaged over 512 scans (range: 600-4000 cm^{-1}).

Membrane Flux and Rejection

The membrane disks were placed inside a Millipore (Billerica, MA) 8010 stirred filtration cell which was pressurized using nitrogen. The cell was filled with a 50% ethanol/water solution and pressurized to 1.4 bar and the permeate outlet opened for 10 minutes in order to wet the membrane. The membrane was removed, washed twice with DI water, and then reassembled into the stirred cell. The cell was then filled with a DI water and pressurized to 1.4 bar and the permeate outlet opened for 10 minutes to flush any remaining ethanol/water from the membrane. The membrane was then submerged in DI water and allowed to rest for 2 hours. After 2 hours, the filtration cell was filled with feed solution carefully to prevent any air bubbles from entering the cell or the feed line, and then pressurized to 3.1 bar. The membranes were allowed to equilibrate for 3 minutes with the permeate line closed. The permeate line was then opened and allowed to flow for 3 minutes before measurements began. Permeate was collected for a given amount of time or until a specified amount of permeate had been obtained. Either three or five

measurements were taken for each filtration run. The membrane was then removed, washed thoroughly with DI water, and returned to storage. Two different feed solutions were used: DI water and a 3.25% w/w mixture of 20 μm neutrally-buoyant polyamide particles plus 0.02% w/w hand soap to minimize particle aggregation. Rejection tests were performed using the latter feed solution. Rejection was calculated as

$$R = 1 - (\frac{c_p}{c_f}) \quad (1)$$

where R is the rejection and c_p and c_f are the concentration of the permeate and the feed, respectively. Both flux and rejection were tested with and without the alternating magnetic field present for base and modified membranes.

Particle Imaging Velocimetry (PIV)

PIV is an optical method of fluid visualization. The fluid is seeded with tracer particles which follow the flow dynamics. It is the motion of these seeding particles that is used to calculate velocity information of the flow being studied [16]. By recording the movements of these particles, the time-resolved flow patterns and velocity vectors of the fluid can be determined. In the presence of an oscillating magnetic field with a specific frequency or frequency range, the magnetic particle capped polymer brushes on the membrane surface will induce mixing at the membrane surface. This can be observed by studying the flow patterns of the fluid immediately next to membrane surface with and without an oscillating magnetic field.

A time-resolved PIV system (Lavision Inc., Goettigen) was used. The membranes were placed in a 90 mm diameter glass Petri dish. The Petri dish was filled with the mixture of DI water, 20 μm polyamide particles, and hand soap. It is the movement of the polyamide particles that is tracked. A green laser (527 nm) illuminated the fluid above the membrane. A high-resolution lens and camera yielded an observable area of 400 μm x 400 μm at maximum resolution. The camera was focused on a two-dimensional plane, roughly 5 mm thick observable area, directly above the surface of the membrane. By capturing the light reflected off of the dispersed particles in the fluid, velocity fields were calculated for this two-dimensional plane. A permanent neodymium-iron-boron magnet was attached to the shaft of a variable speed motor and placed underneath the Petri dish. Observations were made at various motor speeds, including zero. Varying motor speeds generated rotating magnetic fields with different frequencies, which excited the polymer brushes on the membrane at a frequency equal to that of the rotating motor.

Results and Discussion

Theoretical Correlation between Magnetic Nanoparticle Size and Coating Thickness, and the Oscillation Frequency of the External Field

Under an external magnetic field, magnetic particles will experience a torque and a force as shown in Equations (2) and (3), respectively:

$$\vec{\tau} = \vec{\mu} \times \vec{B} \quad (2) \qquad \vec{F} = (\vec{\mu} \cdot \vec{\nabla})\vec{B} \quad (3)$$

where $\vec{\mu}$ is the magnetic moment and $\vec{B}$ is the external field. The resulting torque on the magnetic nanoparticles will cause the alignment of the magnetic moments with the external magnetic field. In addition, the force exerted on the particles will cause them to move in the direction of the gradient. In an alternating magnetic field, the magnetic particles will move and/or rotate in response to the changing field.

Superparamagnetic particles exhibit no remanence once the external magnetic field is removed, as the magnetic dipoles are dispersed by Brownian and Néel relaxations, described by times τ_B and τ_N, respectively [17,18]. Brownian relaxation occurs as the particles try to align their magnetic moments to the external magnetic field by physical rotation. Néel relaxation is caused by the rotation of magnetic moments within the particles themselves without any physical movement of the particles. Brownian relaxation is desired since it will lead to the physical rotation of the magnetic nanoparticles attached to the ends of the polymer brush. Further, heat loss will be minimized if operated off Néel relaxation resonance frequency. The two relaxation times depend on particle diameter differently

$$\tau_B = \frac{3V_H\eta}{k_BT} \qquad (4) \qquad\qquad \tau_N = \tau_0 e^{\frac{KV}{k_BT}} \qquad (5)$$

where V_H and V are the hydrodynamic and magnetic volumes of the nanoparticles respectively, η is the viscosity of the solution, K is the effective anisotropy constant, k_B is the Boltzmann constant, and T is the absolute temperature in Kelvin. Since the relaxation times depend strongly on hydrodynamic and magnetic volumes of the nanoparticles (Brownian depends linearly, Néel exponentially) the two relaxation mechanisms will dominate at different particle sizes. The hydrodynamic volume includes volumes of both the magnetic particle and its protective coating; whereas, the magnetic volume is the volume of the magnetic part of the nanoparticle only.

In addition to the torque, which causes the magnetic moments to align with the external field, the magnetic force acting on the nanoparticle will also cause the particle to move. This magnetic force induces lateral movement of the magnetic nanoparticles and the attached nanobrush in the direction of the gradient. Further the moving nanoparticles will also experience a viscous drag force given by the expression: $F_d = 6\pi\eta R\Delta\nu$, where R is the particle radius, $\Delta\nu$ is the relative linear velocity between the magnetic particle and the solution, and η is the viscosity of the solution. The dipolar interaction between the nanoparticles is weak and can be neglected due to its rapid decay as the particle distance increases. The lateral distance moved is strongly dependent on the gradient, the intrinsic magnetic moment, the switching frequency (i.e. time for particle movement in one direction) and the viscous drag force. For a fixed external field gradient and particle magnetic moment, the speed and distance of the movement by the magnetically activated nanobrush will be strongly dependent on the oscillating frequency.

Both the Brownian and Néel relaxation times as shown in Figures 4 and 5 were calculated as a function of the particle size assuming spherical particles according to Equations 4 and 5. Our calculated results demonstrate that Brownian relaxation occurs on the time scale of 0.01 second or faster for nanoparticle size (both magnetic core and

coating layer) between 10 and 30 nm in water. Brownian relaxation time can be further increased by increasing the coating layer thickness alone. On the other hand, Néel relaxation occurs on the scale of seconds or longer for particle sizes (core) larger than 10 nm.

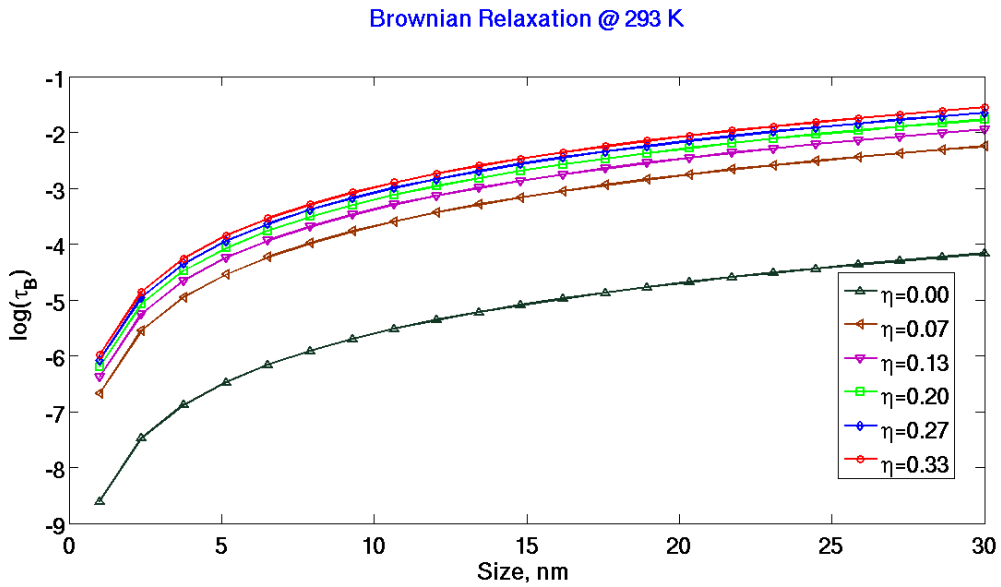

Figure 4. Brownian relaxation time τ_B calculated as a function of solvent viscosity (η) and particle diameter (including magnetic core and coating layer).

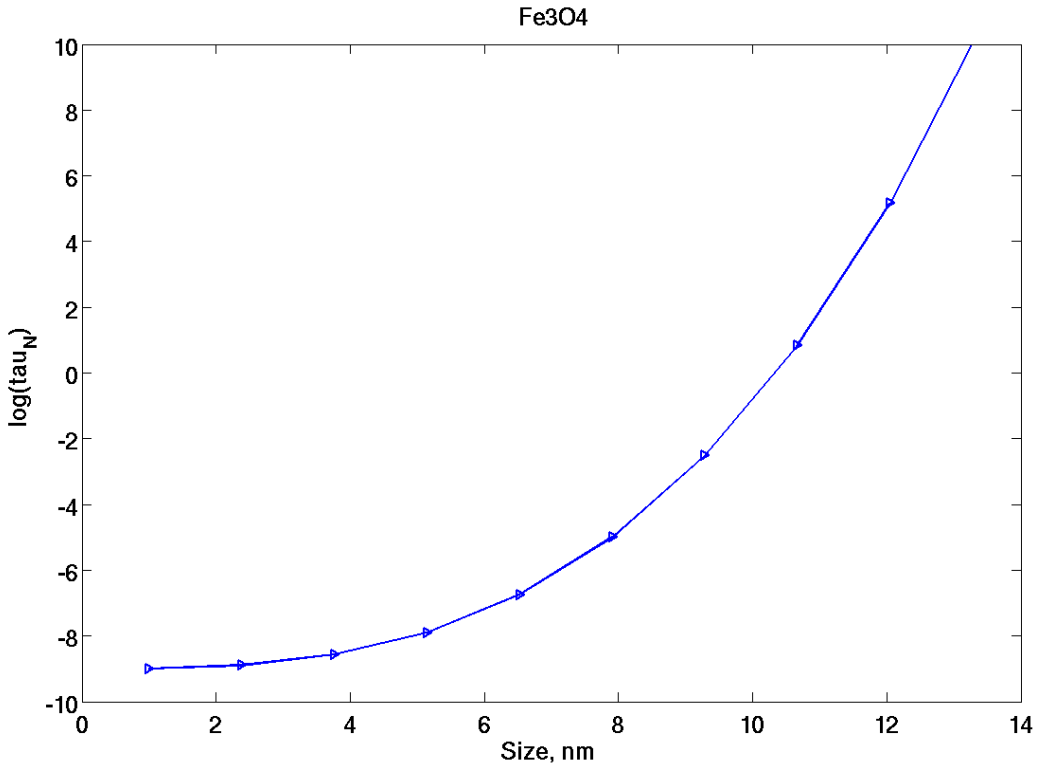

Figure 5. Néel relaxation time vs. particle size (core only) for Fe_3O_4 particles

Alternating Magnetic Field Generator

A system was designed and built to generate an oscillating magnetic field at a desired frequency and intensity. The system consists of two stainless-steel core solenoids, which will power alternatively, on either side of the filtration cell. A computer-operated programmable logic controller (PLC) controlled the rate at which the two solenoids receive power by alternatively activating two solid state relays. This determines the frequency of the alternating of the magnetic field. The solenoids were powered by an Agilent Technologies (Santa Clara, CA) 20V, 25A power supply. Both the strength and frequency of the magnetic field can be adjusted. A schematic of the apparatus is shown in Figure 6. This system was used to generate an oscillating magnetic field for all the filtration experiments.

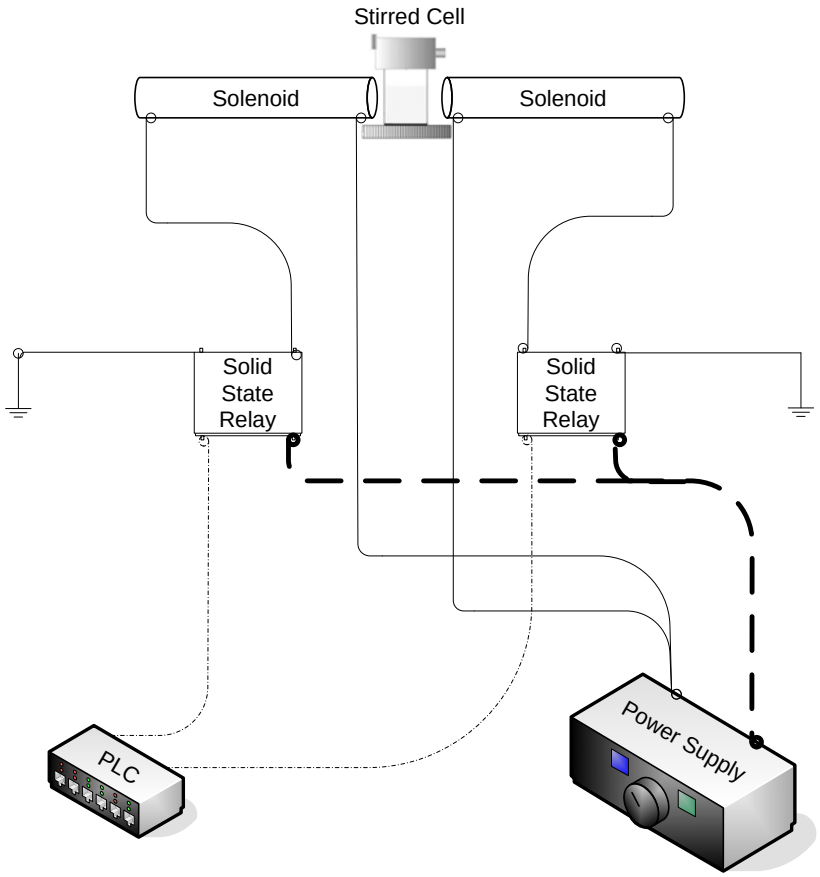

Figure 6. Schematic of alternating magnetic field apparatus.

UV-initiated Grafting

Spectroscopy

Three different sets of modified membranes were created by grafting acrylic acid from the surface of NF 270 membranes: 1% acrylic acid for 15 minutes and 2% acrylic acid for 10 and 15 minutes (labeled **1:15, 2:10**, and **2:15**, respectively). The superparamagnetic nanoparticles were covalently bound to the resulting polyacrylic acid (pAA) brushes

through an amide linkage. Grafting of pAA brushes was confirmed using two types of spectroscopy.

ATR-FTIR spectra in the range 1800 to 1400 cm^{-1} are shown in Figure 7. The control and modified membranes show a number of peaks characteristic of the NF 270 membrane[19]. Peaks at 1584, 1503 and 1487 cm^{-1} indicate the presence of the polysulfone interlayer. A rather broad amide I peak is observed around 1650 cm^{-1}. The modified membranes contain a new peak at approximately 1710 cm^{-1} corresponding to C = O vibration of the carboxylic groups indicating the attachment of poly acrylic acid nanobrushes. The intensity of the peak increases with increasing monomer concentration used during polymerization and UV reaction time. These results suggest that using higher monomer concentrations and longer reactions times lead to greater grafting of acrylic acid monomers from the membrane, as expected.

High resolution XPS data from carbon 1s are shown in Figure 8. The large peak at a binding energy of 284.8 eV corresponding to hydrocarbons represents the majority of the carbon atoms. However modified membranes show a clear carboxylic carbon peak at approximately 288 eV. The intensity of the peak increases with increasing monomer concentration used during polymerization and UV reaction time in agreement with the ATR-FTIR data. Figure 8 also indicates the existence of an amide peak (288.2 eV), amine peak (286 eV), and small carboxylic carbon peak in the base membrane corresponding to the topmost polyamide layer and the existence of a low concentration of residual carboxylic groups in the polyamide layer, as discussed in previous literature [20, 21].

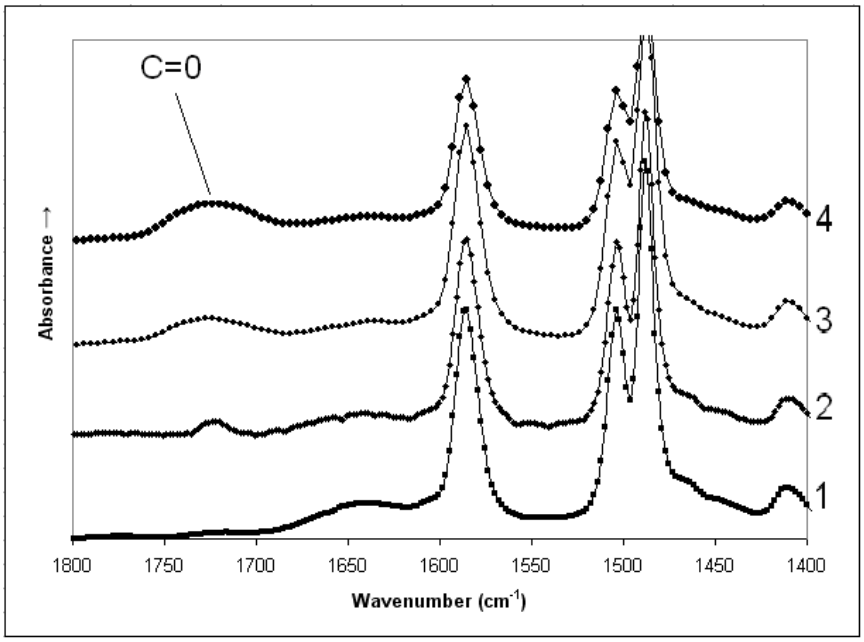

Figure 7. ATR-FTIR spectra for 1) unmodified membrane; 2) 1% acrylic acid, 15 minutes (**1:15**); 3) 2% acrylic acid, 10 minutes (**2:10**); and 4) 2% acrylic acid, 15 minutes (**2:15**). Increasing the height of the carbonyl peak (~1710 cm^{-1}) corresponds to the increased grafting of pAA.

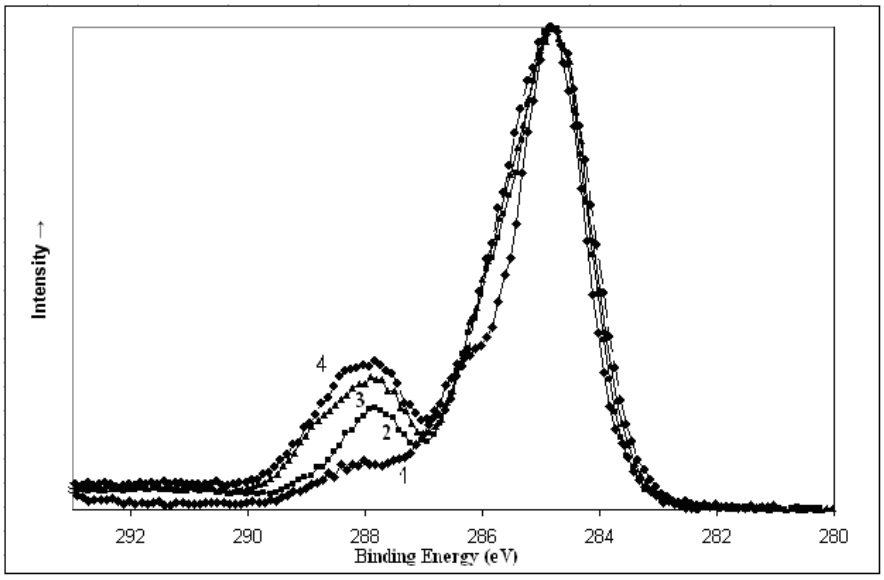

Figure 8. XPS spectra for 1) unmodified membrane; 2) 1% acrylic acid, 15 minutes (**1:15**); 3) 2% acrylic acid, 10 minutes (**2:10**); and 4) 2% acrylic acid, 15 minutes (**2:15**). Increasing the height of the carbonyl peak (~288 eV) corresponds to the increased grafting of pAA.

Permeate Flux

Permeate flux, for DI water for each of the three UV modification conditions as well as an unmodified control membrane is presented in Figures 9-12. As expected membrane modification leads to a decrease in permeate flux. The polymerization condition that leads to the greatest addition of polymer to the membrane surface (**2:15**) leads to the greatest decrease in permeate flux compared to the base membrane. For the control membrane, Figure 9, the flux is independent of the alternating magnetic field as expected.

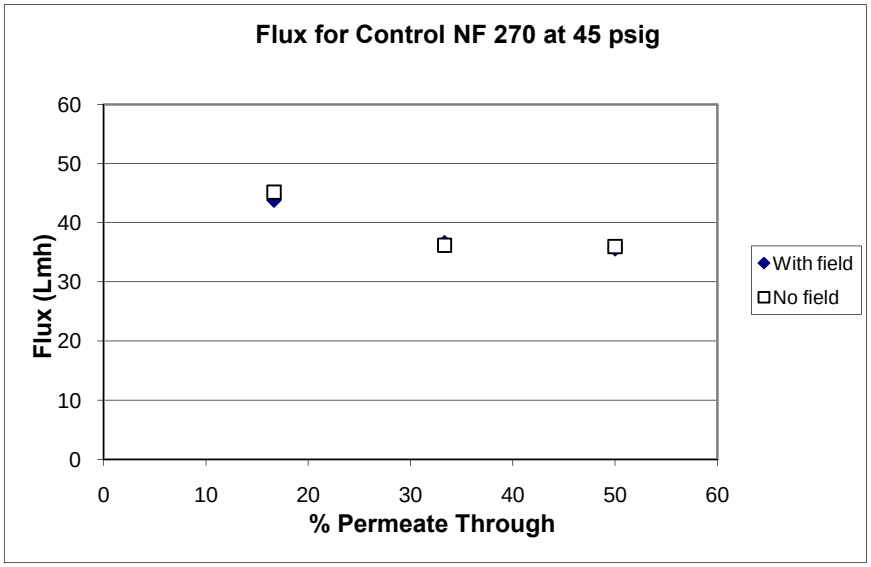

Figure 9. Flux for unmodified NF 270 membrane at 45 psig (3.1 bar).

Figures 10-12, on the other hand, show that the flux for the modified membranes depends on the external magnetic field with a frequency of 100 Hz. This result seems remarkable

for a feed stream consisting of DI water. However it is likely that in the absence of an oscillating magnetic field, the polymer brushes are relaxed and exist in a more coiled conformation. However in the presence of an oscillating magnetic field the brushes are more extended leading to a decrease in the resistance to permeate flow due to the grafted polymer brush layer. The frequency used appears to agree with Brownian relaxation mechanism for the physical rotation of the magnetic nanoparticles to align with the external field.

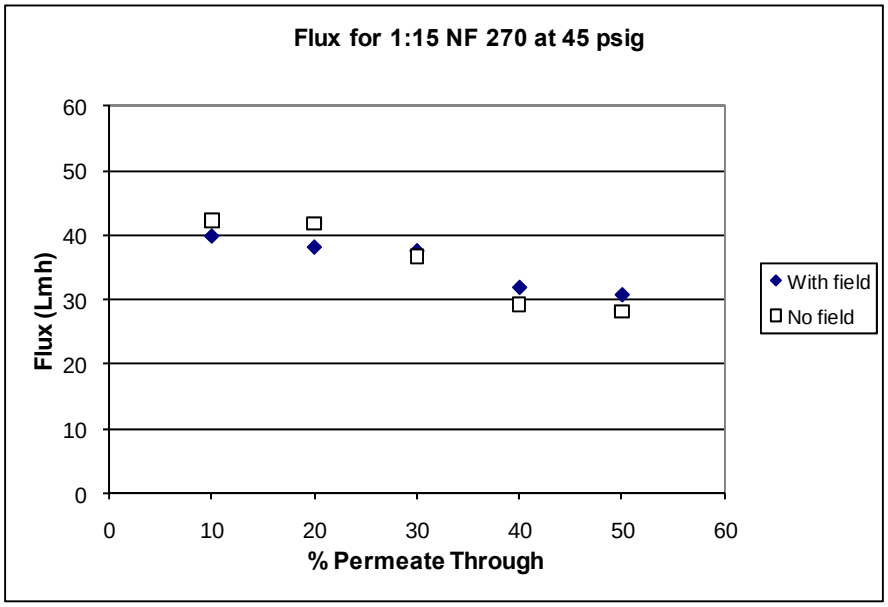

Figure 10. Flux for 1%, 15 minutes (**1:15**) modified membrane at 45 psig (3.1 bar).

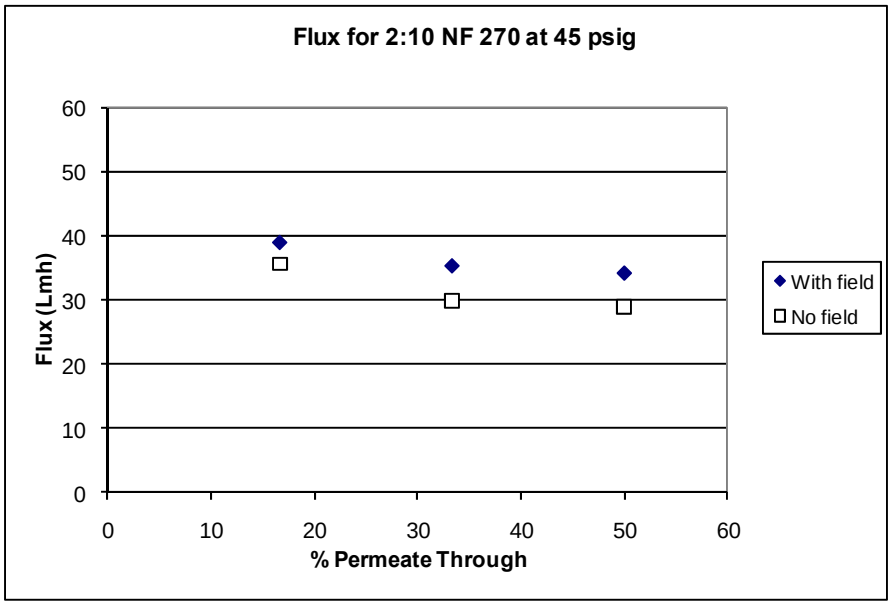

Figure 11. Flux for 2%, 10 minutes (**2:10**) modified membrane at 45 psig (3.1 bar).

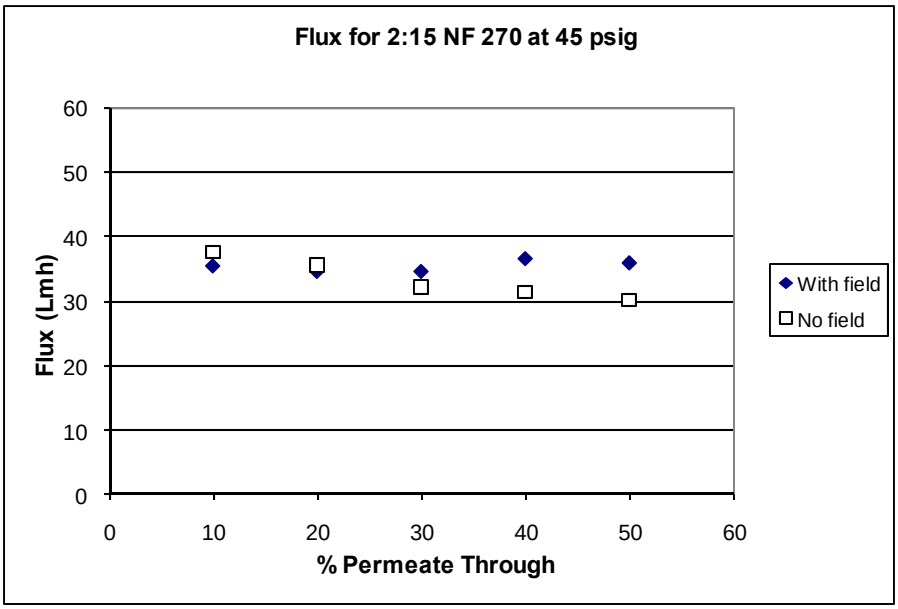

Figure 12. Flux for 2%, 15 minutes (**2:15**) modified membrane at 45 psig (3.1 bar).

Membrane Rejection

Figures 13-16 give rejection results for a model feed stream consisting of DI water, hand soap and polyamide particles. Rejection is determined using Equation 1. Given that the nanofiltration membranes will reject the polyamide particles we are measuring passage of the hand soap during dead end filtration. Figure 13 gives results for the control unmodified base membrane. As expected the presence of an oscillating magnetic field has no effect on the rejection behavior of the control membrane. Further rejection of the hand soap decreases with time due to increased concentration of the hand soap in the feed reservoir as permeate is removed.

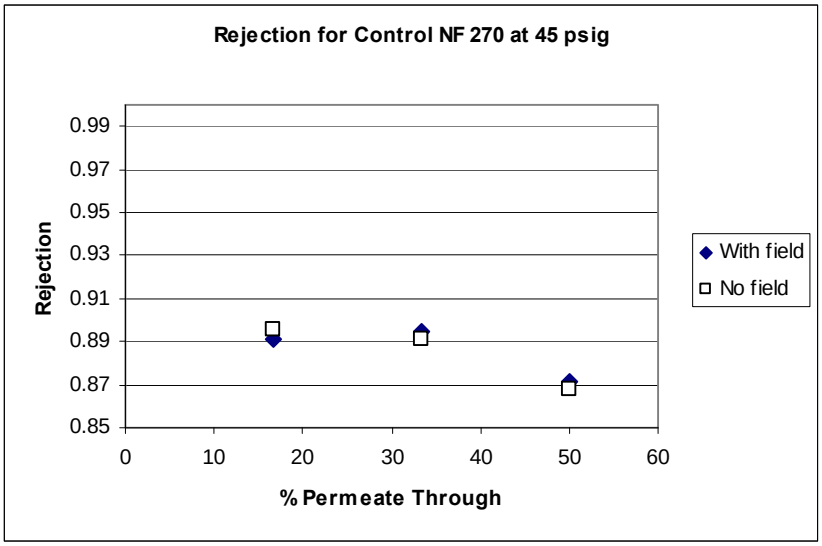

Figure 13. Rejection of polyamide particles and hand soap in DI water for control unmodified base membrane at 45 psig (3.1 bar).

The rejection behavior of the modified membranes is very different (Figures 14-16). In these figures the rejection behavior of the unmodified membrane is included for comparison. As can be seen rejection is increased due to the presences of the grafted polymer brush layer. This is in agreement with the reduced permeate fluxes observed after membrane modification. Grafting leads to tightening of the membrane pore structure. More striking is the fact that rejection is further enhanced for the modified membranes in the presence of an oscillating magnetic field. We contend that the movement of the magnetically activated brushes leads to a disruption of the concentration boundary layer which results in enhanced rejection of the hand soap. The movement of the magnetically active brushes leads to enhanced rejection.

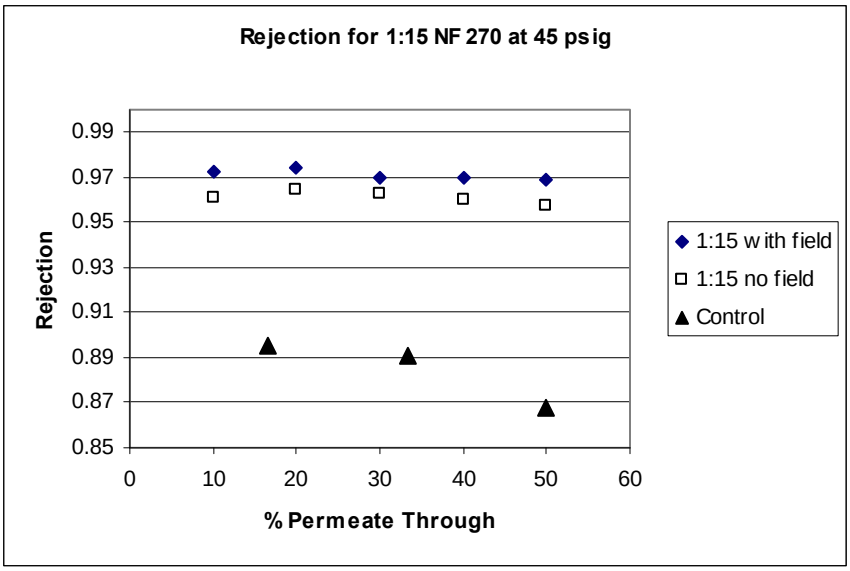

Figure 14. Rejection of polyamide particles and hand soap in DI water for 1% acrylic acid, 15 minute (**1:15**) membrane at 45 psig (3.1 bar).

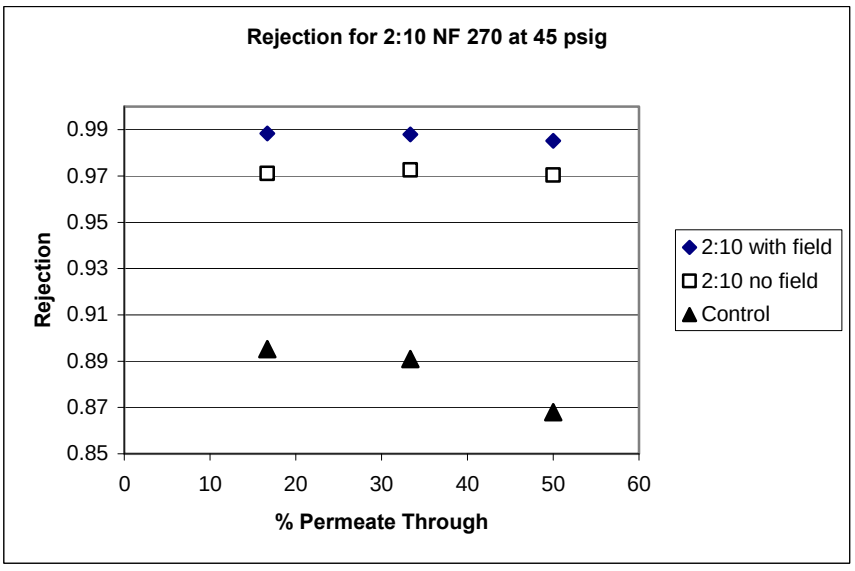

Figure 15. Rejection of polyamide particles and hand soap in DI water for 2% acrylic acid, 10 minute (**2:10**) membrane at 45 psig (3.1 bar).

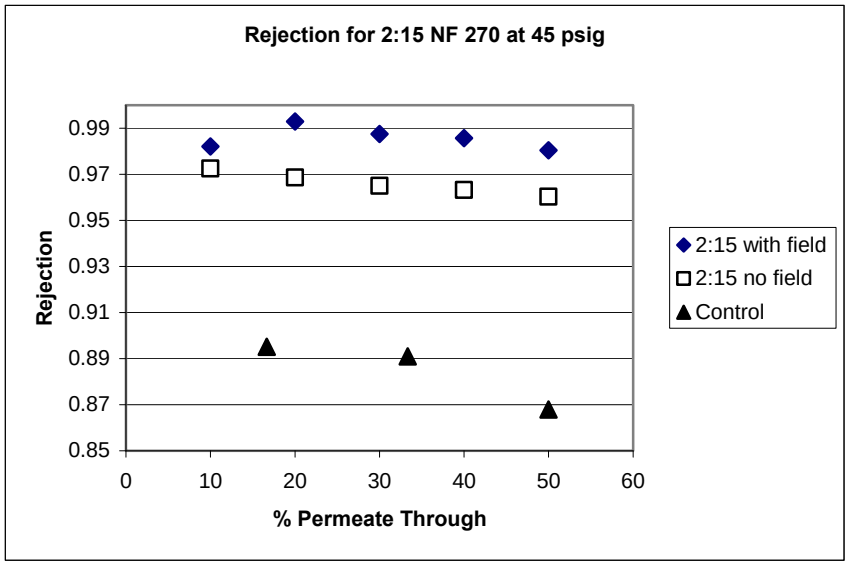

Figure 16. Rejection of polyamide particles and hand soap in DI water for 2% acrylic acid, 15 minute (**2:15**) membrane at 45 psig (3.1 bar).

ATRP Grafting

ATRP grafting was studied as an alternative way to graft polymer brushes on the membrane surface. ATRP is a highly controllable, "living" polymerization. Using ATRP, it is possible to finely control the polymer grafting density and polymer chain length. In addition we ensure that nanoparticles are attached only to the ends of the polymer brushes.

Spectroscopy

HEMA brushes were grafted from the surface of NF 270 membranes using ATRP; ATRP reaction time was 4.5 hours. The Gabriel Synthesis reaction was then used to convert the alkyl halide end group of the brushes into primary amines before attaching the magnetic nanoparticles. The amine groups of the HEMA brushes were bonded to the carboxylic acid groups on the coatings of the nanoparticles through the creation of an amide bond.

XPS was used to verify HEMA grafting and conversion of the bromine functional group to an amine using the Gabriel Synthesis. Figure gives a high-resolution spectrum of the 1s carbon region for various stages of polymerization. The decrease in peak height associated with C-C and C-H bonds (284.5 eV) after initiation and HEMA grafting suggests that linear polymer brushes are indeed being grafted. This is because XPS data were collected from the topmost layers only. Total carbon bond count should decrease with linear chain polymerization because the density of carbon would decrease due to the limited number of polymerization sites on the membrane surface.

The peak associated with the C-OH bond appears at ~286.4 eV after HEMA polymerization. This functionality is not present in large numbers in the top layer of the base membrane, which is composed predominantly of carbonyl groups. The appearance and growth of this peak with polymerization further support that HEMA has been

successfully grafted from the membrane surface. Finally, the peaks at 288 and 289 eV are also of interest. These two peaks correspond to carboxylic acid (HO-C=O) and ester functional groups (O-C=O) respectively. As mentioned previously, the topmost surface of NF 270 membranes is covered with carbonyl groups. These excite at 288 eV resulting in a strong peak for both the base and initiated membranes. After polymerization, however, the peak at 288 eV reduces to almost zero whereas the peak at 289 eV becomes quite defined. Since all of the carbonyl groups present in the HEMA brushes are esters, these carbonyls were excited at 289 eV rather than 288 eV. Thus, the presence of HEMA growing from the membrane surface is further confirmed.

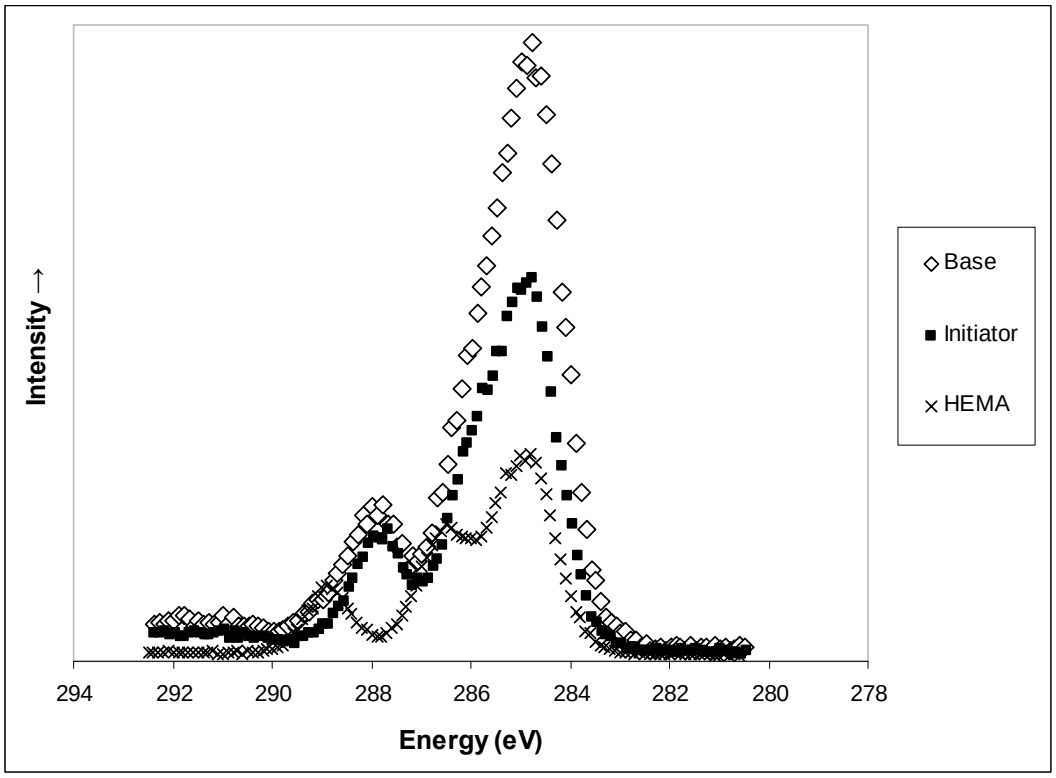

Figure 17. High-resolution XPS spectra at the carbon region during various stages of ATRP polymerization (base membrane, after initiation, and after HEMA grafting).

Figure 17 confirms the successful HEMA grafting from the membrane surface. The next step in the modification procedure was to convert the bromine functionality on the end of each polymer chain to a primary amine in order to chemically attach the superparamagnetic nanoparticles. Figure 18 is a high-resolution XPS spectrum for the nitrogen region. The amine peak (399.5 eV) is present for the unmodified membrane due to the top layer of polyamide in base membrane. This peak is suppressed somewhat during initiation and then completely disappears during HEMA grafting. This suggests that the HEMA polymer chains are of significant length (>10nm) that XPS cannot detect the polyamide layer of the base membrane. After the Gabriel Synthesis is performed, the peak appears again, thus confirming the generation of amine functionalities on the end of the HEMA polymer brushes. With the ends of the polymer chains converted to amines, nanoparticle attachment can be subsequently carried out.

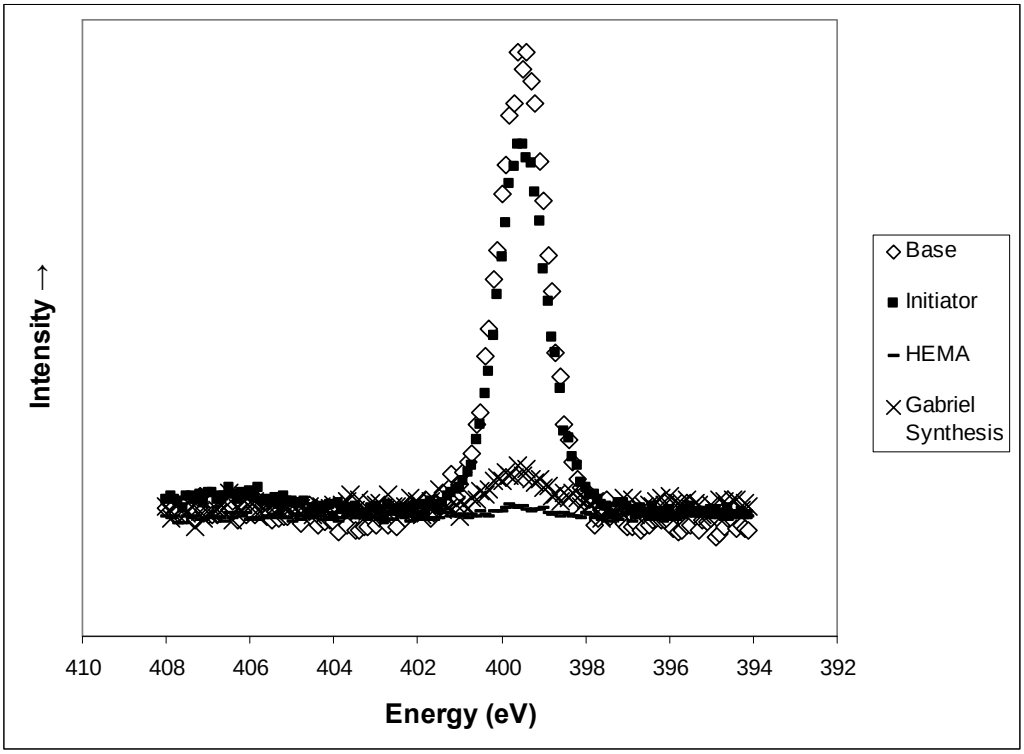

Figure 18. High-resolution XPS spectra at the nitrogen region during various stages of polymerization (unmodified base membrane, after initiation, after HEMA grafting, and finally after Gabriel Synthesis). The amine peak is suppressed during HEMA polymerization, but then reappears after performing the Gabriel Synthesis.

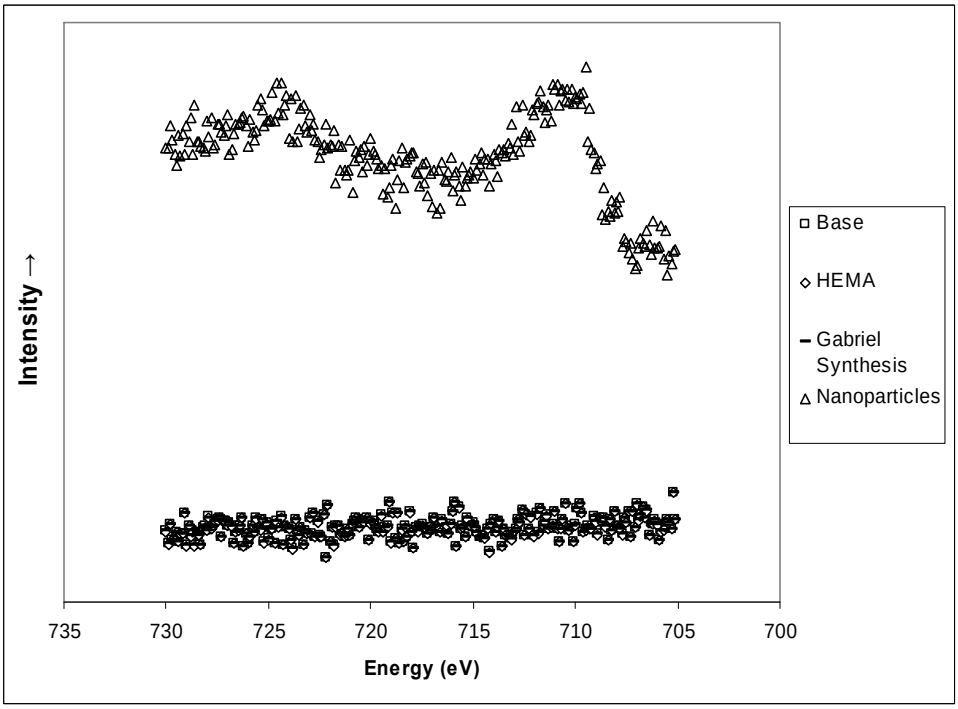

Figure 19. High-resolution XPS spectra at the Fe region during various stages of polymerization. The two peaks associated with Fe(II) (710 and 725 eV) are only present after the attachment of the iron oxide nanoparticles on the polymer brushes.

XPS was also used to verify the presence of iron oxide nanoparticles after modification, see Figure 19. High-resolution scans of the iron region were performed for unmodified membranes and those in various states of modification. No iron was detected until after nanoparticle attachment. After nanoparticle attachment, strong peaks appeared at 710 and 725 eV, which are associated with Fe(II), confirming the presence of iron.

Permeate Flux

Figure 20 shows permeate as a function of time at a constant pressure of 45 psig (3.1 bar) using DI water. The results are similar to those obtained for membranes modified using UV initiated polymerization. The presence of an oscillating magnetic field with 100 Hz has no effect on the permeate flux for the unmodified base control membrane. Surface modification of the base membrane leads to a decrease in permeate flux due to the added resistance to permeate flow from the grafted polymer brush layer. In the presence of an oscillating magnetic field, the permeate for DI water for the modified membrane is higher than the permeate in the absence of an oscillating magnetic field. We contend that in the presence of an oscillating magnetic field the magnetically activated brush adopt a more stretched conformation which reduces the resistance to permeate flow from the grafter polymer brush layer.

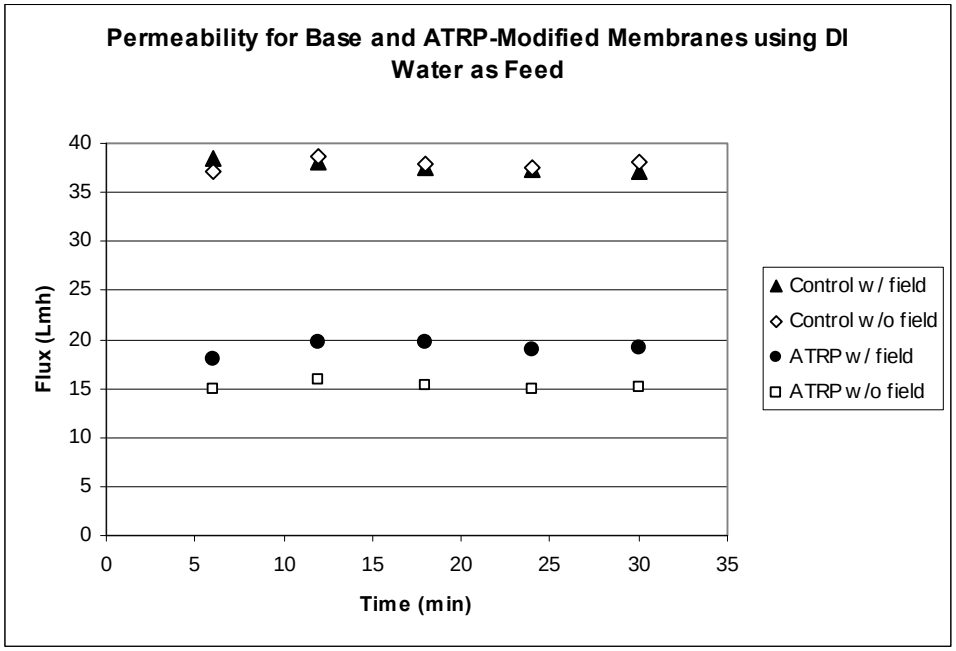

Figure 20. Membrane flux of DI water, or flux, plotted against time at 45 psig (3.1 bar). Modification reduces flux by roughly 35%.

Once the base DI water flux of the ATRP modified membranes had been established, see Figure 20, the membranes were tested using the mixture of hand soap and polyamide particles described previously. As can be seen in Figure 21 the flux through the membrane without a magnetic field decreases greater than 50% compared to when DI water was used. This decrease is due to concentration polarization of the oily hand soap film. With the magnetic field, however, the flux through the membrane is improved by roughly 40% compared to without the field. The concentration polarization is broken up by the mixing resulting from the movement of the polymer brushes thus increasing flux.

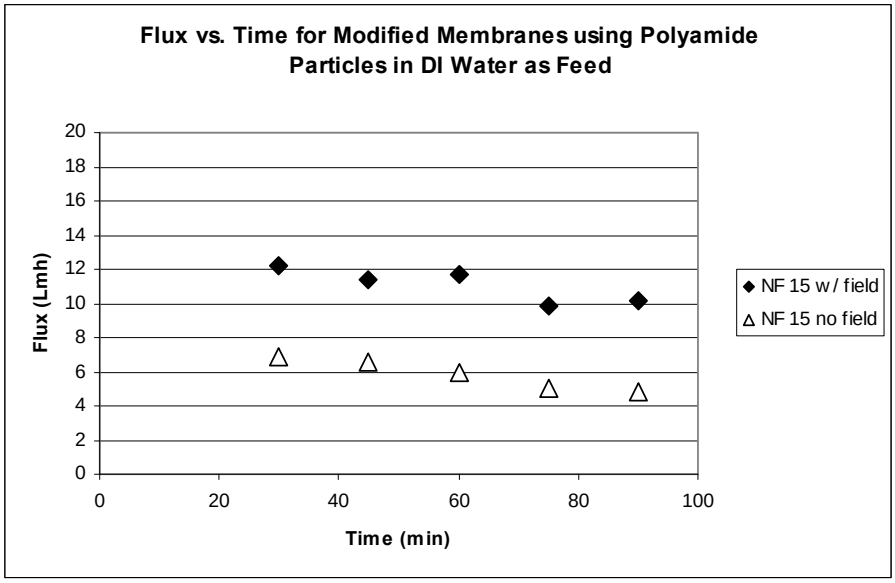

Figure 21. Membrane flux during filtration of mixture of polyamide particles and hand soap in water, plotted against time at 45 psig (3.1 bar). Flux clearly increases in the presence of an oscillating field.

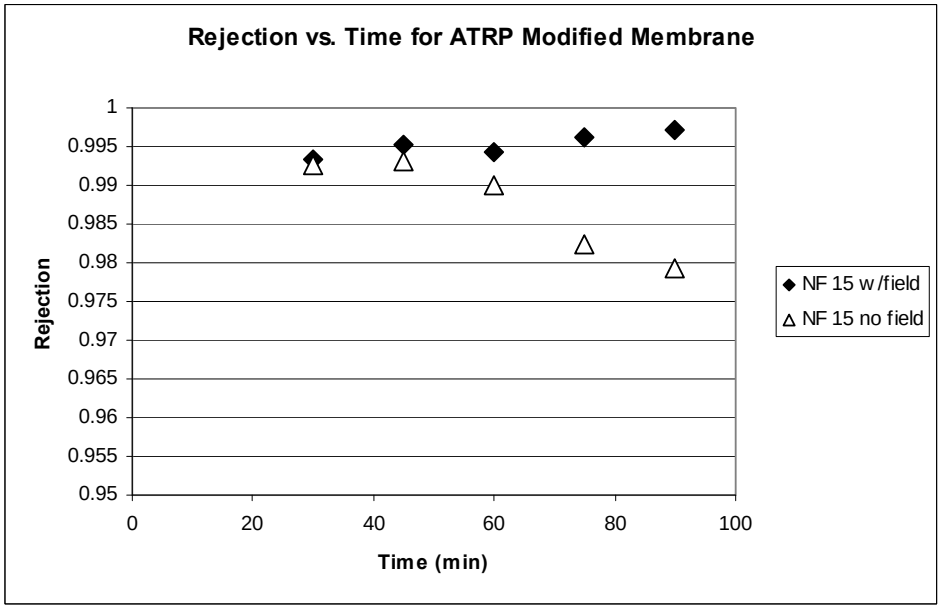

Figure 22. Rejection of polyamide particles and hand soap in water mixture. Both rejections begin extremely high; however, in the field, the rejection is relatively constant (and slightly increases), but the rejection without the field steadily decreases.

Membrane Rejection

Figure 22 gives the rejection data for the ATRP modified membranes. The results are similar to the results obtained for membranes modified using UV initiated polymerization but are more dramatic. In the presence of an oscillating magnetic field a very high level of rejection is maintained throughout the experiment. We contend that this is due to disruption of the concentration boundary layer by the movement of the magnetically

activated polymer brushes. Since the ATRP protocol ensures that nanoparticles are only attached to the ends of the polymer brushes, it is likely that the movement of the brushes is greater leading to the more dramatic effect (comparison between Figures 22 and 14-16)

PIV Results

Unmodified and modified NF 270 membranes were each observed in the PIV setup with and without a magnetic field present. The rotational speed of the shaft, upon which the permanent magnet was placed, was varied to generate 3 different time-alternating magnetic fields. The motor was increased in increment of 30% of total output resulting in four oscillating frequencies: 0, 9, 22, and 30 Hz. These frequencies are much less than the Brownian relaxation frequency. Therefore, only the lateral movement by the magnetic nanobrushes due to the magnetic force is considered in the analysis below. The PIV results are presented in Figure 23.

As can be seen in Figure 23, the fluid behavior for the unmodified membrane is well-behaved and orderly. The modified membrane at a rotational speed of 0 Hz is similarly ordered. For 9 and 22 Hz, however, the fluid behavior for the modified membrane is noticeably different compared to the 0 Hz case. The alignment of the polymer brushes with the oscillating magnetic field has caused mixing of the fluid above the membrane surface leading to chaotic fluid behavior. This mixing is apparent in the orientation of both the red field lines and the velocity vectors.

Interesting to note is the increased fluid mixing for 9 Hz compared to 22 Hz. It is believed that this is due to the lateral distance traveled by the polymer brushes. That is, the faster the field is moving, the less time the polymer brushes travel in a given direction. This shortened time means that the brushes will not be able to cover as much distance during the lateral movement, thereby resulting in less mixing. This also explains why the 30 Hz data for the modified membrane appears so similar to the 0 Hz data. The magnetic field is switching so quickly that the brushes can only travel a very short distance in a given direction. The distance traveled is so short, that the resulting small amount of mixing seems to not affect the fluid. Mathematically, the distance covered by the polymer brush/nanoparticle structure is inversely related to the frequency squared, as shown in Equation 6.

$$d \sim \frac{F}{m}\left(\frac{1}{f^2}\right) = w\left(\frac{1}{f^2}\right) \tag{6}$$

Here F is the force the magnetic field exerts on the magnetic nanoparticles and m is the mass of the magnetic polymer nanobrush (here labeled as the constant w). The distance (d) travelled is directly related to the frequency of the field (f). This can be used to explain the results in Figure 23. The distance traveled by the brushes at 9 Hz is $\frac{w}{9^2}$ or $\frac{w}{81}$. By contrast, the maximum distances traveled for the same brush, in the same field, at 22 Hz and 30 Hz are only $\frac{w}{484}$ and $\frac{w}{900}$, respectively. The dramatically shortened distances at these higher frequencies would result in less turbulence created in the fluid. In fact, the resulting mixing at 30Hz is so small, that it appears to have no effect on fluid behavior.

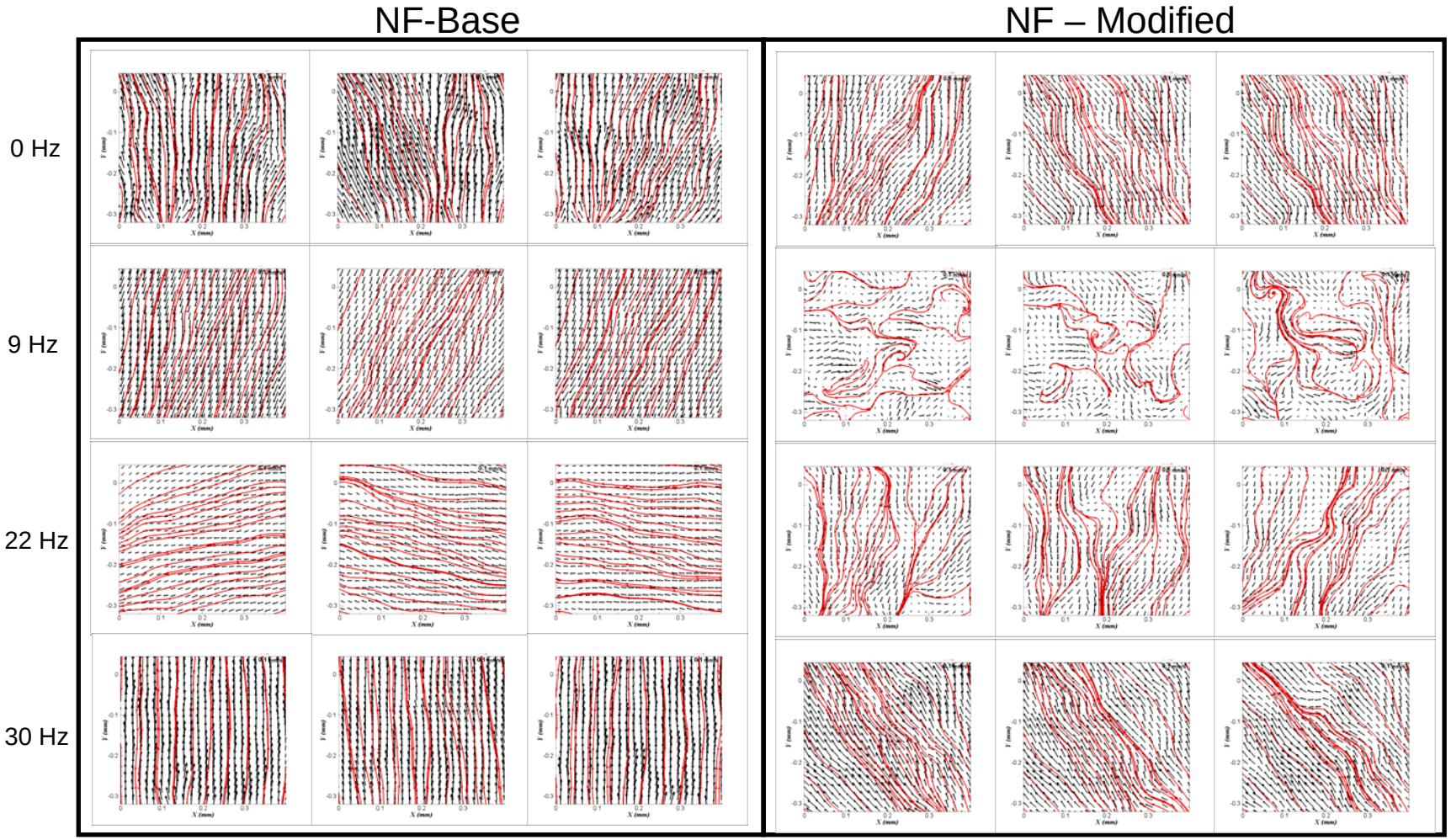

Figure 23. Series of 3 successive PIV vector diagrams for magnet rotation speed of 0, 9, 22, and 30 Hz. Each vector diagram is averaged over 1ms of time; therefore, 3 ms time is shown for each of the four frequencies. The most turbulence due to the movement of polymer brushes in the magnetic field can be seen for the 9 Hz sample.

Comparison between UV Initiated Polymerization and ATRP

In this work we have investigated the use of two different polymerization methods to grow polymer brushes from the surface of nanofiltration membranes. For both methods, surface characterization indicates attachment of polymer brushes from the surface of the membrane and attachment of nanoparticles to these polymer brushes. For both polymerization methods, grafting polymer brushes from the surface of the membrane leads to a decrease in permeate flux due to the increased resistance to permeate flow as a result of the presence of the polymer brush layer. Dead end filtration results for DI water and DI water containing hand soap and polyamide particles indicate higher permeate fluxes and higher rejection of the hand soap in the presence of an oscillating magnetic field for the modified membranes. For base membranes the presence of an oscillating magnetic field has no effect on permeate flux or rejection.

The advantages of the UV initiated polymerization method stems from the fact that it is simple, quick and routinely used in industry to modify membrane surfaces. On the other hand, the ATRP method is far more complicated, time consuming and is not currently used in industry to modify commercial membrane surfaces. In addition, we show that the UV initiated polymerization method is successful in creating magnetically activated membranes.

Nevertheless ATRP offers a number of unique advantages over UV initiated polymerization. ATRP is a living polymerization process. The polymerization may be stopped and later restarted. By varying the amount of Cu (I) to Cu (II) the reaction rate may be controlled[22,23,24,25,26]. Slower reaction rates result in lower polydispersity in the polymer brush lengths. Though not studied in this SEED proposal, obtaining uniform polymer brush with a nanoparticle attached to the end of the brush is likely to improve mixing compared to a range of brush lengths. Further, the density of brushes may be varied by varying the initiator density independent of the brush polydispersity.

Here we have developed a protocol for attaching nanoparticles to only the ends of the polyHEMA brushes grown from the membrane surface using ATRP. Our permeate flux and rejection results indicate that the ATRP method leads to membranes that show better performance (flux and rejection) than the UV initiated polymerization method in the presence of an oscillating magnetic field. We believe this is partly due to the fact that the brushes are likely to be more uniform in length and partly to the fact that the magnetic particles are only attached to the brush ends using ATRP scheme.

Our results indicate that ATRP offers a number of advantages over UV initiated polymerization. In particular in a future full proposal one could investigate the effect of brush length and polydispersity independent of brush density on the magnetic response of the membrane. The effect on membrane performance could easily be determined through dead end and tangential flow filtration experiments. In addition, the PIV system we have developed will allow easy visualization of the mixing induced by the magnetically activated polymer brushes.

Conclusions and Implications for Future Research

The conclusions of this proof of concept project are as follows:

Polymer brushes have been successfully grown from the surface of nanofiltration membranes using UV initiated polymerization and atom transfer radical polymerization. Superparamagnetic nanoparticles may be attached to these polymer brushes. The magnetically responsive polymer brushes move in an oscillating magnetic field. Movement of the magnetically responsive brushes leads to mixing at the membrane surface. A solenoid system was established to produce an oscillating magnetic field that activated the magnetically responsive membranes during filtration. We show that for magnetically responsive membranes the presence of an oscillating magnetic field improves membrane performance under certain frequencies. In particular, for dead end filtration of DI water and DI water containing polyamide particles and hand soap, we observe an increase in permeate flux and rejection of the hand soap in the presence of an oscillating magnetic field. Theoretical calculations also predict that the superparamagnetic particles used here will move in an oscillating magnetic field. Finally we show that the oscillation frequency of the field affects the level of mixing. This agrees with theoretical predictions.

We have shown that magnetically activated membranes may be developed and could represent a new class of fouling resistant membranes that are ideally suited for treatment of oily waters. Importantly we have successfully addressed the critical issues that represented the maximum risk in a full proposal. Follow-on work, aimed at developing a practical solution for treatment of bilge and other oily waters, will include the following further research and development.

Design and fabrication of a tangential flow filtration cell for testing magnetically responsive membranes in tangential flow filtration. The current solenoid system we have developed is capable of testing membranes with surface areas up to 100 cm^2. Fabrication of a tangential flow filtration cell is relatively simple.

In collaboration with membrane manufacturers and the Navy, it will also be important to develop a scaled down filtration module that accurately represents the geometry and operating conditions for testing real bilge waters. These results will be critical in determining the actual performance expected on naval ships. Membrane capacity, throughput, time between membrane cleaning, and possible modifications/simplifications to any pretreatment steps and cleaning protocols currently employed will be investigated.

The above tasks represent the more practical development work that is required in order to further develop this technology. In addition, there are several more fundamental studies that also need to be conducted. In order to optimize the surface modification of membranes, it is important to determine the effect of polymer brush length, brush polydispersity and brush density on the level of mixing obtained. The ATRP method we have developed here is ideal for these studies. In addition it is essential to minimize the number of polymer brushes that attach to a given superparamagnetic particle. If too many polymer brushes attach to a given particle, it will constrict the movement of the particle, thus reducing mixing. The number of brushes that attach to a given nanoparticle may be minimized by carefully controlling brush length and density. In addition we could develop a chemical procedure for capping a fraction of the functional groups

on the nanoparticles, again reducing the possibility of multiple attachments of brushes to a given nanoparticle.

Parallel theoretical calculations will help guide our future experiments. A Computational Fluid Dynamics (CFD) fluid-structure model will be constructed to evaluate mixing and energy consumption characteristics for a given nanobrush length, nanoparticle size, and graft density. Maximum mixing is one of the goals and will be primarily dependent on the size, spacing (density), and length of the brushes, the nanoparticle properties and external field characteristics. Further, these parameters also govern energy usage, and heat production, so optimization requires a method to navigate the parameter space and the ability to predict mixing characteristics for any given configuration. A fluid-structure computational model will be developed using CFD tools to study the mixing characteristics as a function of particle size, spacing, and nanobrush length. We will create 2D and 3D models to input time dependent force and torque on every particle and simulate the ensuing flow fields. The model will enable direct characterization of mixing using Lagrangian analysis of passive markers, and mechanical work done (or mechanical power requirement) by the nanoparticles.

Literature Cited

[1] Gilron, J., Belfer, S., Väisänen, P. & Nyström, M. (2001), Modification of RO membranes for Antifouling Resistance, *Desalination*, 140, 167-179.

[2] Ulbricht, M. & Yang, H. (2005), Porous polypropylene membranes with different carboxyl polymer brush layers for reversible protein binding via surface initiated graft-copolymerization, *Chem. Mater.*, 17, 2622-2631.

[3] Vandevivere, P.C., Bianchi, R. & Verstraete, W. (1998), Treatment and reuse of wastewater from the textile wet-processes industry: review of emergin technologies, *J. Chem. Technol. Biotechnol.*, 72, 289-302.

[4] Tomaszewska, M., Orecki, A. & Karakulski, K. (2005), Treatment of bilge water using a combination of ultrafiltration and reverse osmosis, *Desalination*, 185, 203-212.

[5] Qin, J. Oo, M., Lee, H. & Kolkman, R. (2004), Dead-end ultrafiltration for pretreatment of RO in reclamation of municipal wastewater effluent. *J. Membr. Sci.*, 243, 107-113.

[6] Hu, X., Bekassy-Molnar, E. & Vatai, G. (2004), Study of transmembrane pressure and gel resistance in ultrafiltration of oily emulsion, *Desalination*, 163, 355-360.

[7] Morão, A., Escobar, I., Pessoa de Amorim, M., Lopes, A. & Gonçalves, I.C. (2005), Postsynthesis modification of a cellulose acetate ultrafiltration membrane for applications in water and wastewater treatment, *Environ. Prog.*, 24, 367-382.

[8] Reddy, A., Trivedi, J., Devmurari, C., Mohan, D., Singh, P., Rao, A., Joshi, S. & Ghosh, P. (2005), Fouling resistant membranes in desalination and water recovery, *Desalination*, 183, 301-306.

[9] Kliduff, J., Mattaraj, S., Zhou, M. & Belfort, G. (2005), Kinetics of Membrane Flux Decline: The role of natural colloids and mitigation via membrane surface modification, *J. Nanoparticle Research*, 7, 525-544.

[10] Schlemmer, C., Betz, W., Berchtold, B., Rühe, J. & Santer, S. (2009), The design of thin polymer membranes filled with magnetic particles on a microstructured silicon surface, *Nanotechnology,* 20, 255301.

[11] Hoare, T., Santamaria, J., Goya, G., Irusta, S., Lin, D., Lau, S., Padera, R., Langer, R. & Kohane, R. (2009), A magnetically triggered composite membrane for on-demand drug delivery, *Nano Lett.* 9, 3651-3657.

[12] Edelman, E., Kost, J., Bobeck, H. & Langer, R. (1985), Regulation of drug release from porous polymer matrices by oscillating magnetic fields, *J. Biomed. Mat. Res.*, 19, 67-83.

[13] Tang, C., Kwon, Y. & Leckie, J. (2009), Effect of membrane chemistry and coating layer on physiochemcial properties of thin film composite polyamide RO and NF membranes. II. Membrane physiochemical properties and their dependence on polyamide and coating layers, *Desalination*, 242, 168-182.

[14] Monge, S., Giani, O., Ruiz, E., Cavalier, M. & Robin, J. (2007), A new route for the modification of halogen end groups to amino end-functionalized poly(tert-butyl acrylate)s, *Macro. Rapid Comm.*, 28, 2272-2276.

[15] Hollander, J. & Jolly, W. (1970), X-ray photoelectron spectroscopy, *Acc. Chem. Res.*, 3, 193-200.

[16] Raffel, M., Willert, C., Wereley, S. & Kompenhans, J. (2007), *Particle Image Velocimetry*: *A Practical Guide*, Springer, Berlin.

[17] Singh, H., Laibinis, P. & Hatton, T. (2005). Rigid, superparamagnetic chains of permanently linked beads coated with magnetic nanoparticles. Synthesis and rotational dynamics under applied magnetic fields. *Langmuir*, 21, 11500-11509.

[18] Chung, S.H., Hoffmann, A., Guslienko**,** K., Bader, S., Liu, C., Kay, B., Makowski, L. & Chen, L. (2005). Biological sensing with magnetic nanoparticles using Brownian relaxation, *Journal of Applied Physics*, 97, 10R101.

[19] Mondal, S. & Wickramasinghe, S.R. (2008), Produced water treatment by nanofiltration and reverse osmosis membranes, *J. Membr. Sci*, 322, 162-170.

[20] Kang, G., Liu, M., Lin, B., Cao, Y. & Yuan, Q. (2007), A novel method of surface modification on thin-film composite reverse osmosis membranes by grafting poly(ethylene glycol), *Polymer*, 48, 1165-1170.

[21] Nyström, M., Butylina, S. & Platt, S. (2004), NF retention and critical flux of small hydrophilic/hydrophobic molecules, *Membrane Technology*, 10, 5-8.

[22] Wandera, D., Wickramasinghe, S.R. & Husson, S.M. (2010), Review Stimuli-responsive Membranes, *Journal of Membrane Science*, 357(1-2), 6-35.

[23] Tomer. N., Mondal, S., Wandera, D., Wickramasinghe, S. R. & Husson, S. M. (2009), Modification of Nanofiltration Membranes by Surface-initiated Atom Transfer Radical Polymerization for Produced Water Filtration, *Separation Science and Technology*, 44(14), 3346-3368.

[24] Bhut, B. V., Wickramasinghe, S. R. & Husson, S. M. (2008), Preparation of high-capacity, weak anion-exchange membranes for protein separations using surface-initiated atom transfer radical polymerization, *Journal of Membrane Science*, 325 (1), 176-183.

[25] Singh, N., Chen, Z., Tomer, N., Wickramasinghe, S. R. Soice, N. & Husson, S.M. (2008), Modification of regenerated cellulose ultrafiltration membranes by surface-initiated atom transfer radical polymerization, *Journal of Membrane Science*, 311, 225-234.

[26] Singh, N., Wang, J., Ulbricht, M., Wickramasinghe, S. R. & Husson, S. M. (2008), Surface-initiated Atom Transfer Radical Polymerization: A New Method for Preparation of Polymeric Membrane Adsorbers, *Journal of Membrane Science,* 309(1-2), 64-72.